[16] S. V. Ley, D. K. Baeschlin, D. J. Dixon, A. C. Foster, S. J. Ince, H. W. M. Priepke, D. J. Reynolds, *Chem. Rev.* **2001**, *101*, 53, and references therein.
[17] H. Orth, *Angew. Chem.* **1952**, *64*, 544.
[18] M. E. Furrow, S. E. Schaus, E. N. Jacobsen, *J. Org. Chem.* **1998**, *63*, 6776.
[19] Available from Aldrich in either enantiomeric form.
[20] For similar observations in reactions using dispiroketal-desymmetrized glycolic acid, see; a) G.-J. Boons, R. Downham, K. S. Kim, S. V. Ley, M. Woods, *Tetrahedron* **1994**, *50*, 7157; b) R. Downham, K. S. Kim, S. V. Ley, M. Woods, *Tetrahedron Lett.* **1994**, *35*, 769.
[21] Specific rotations: **21**: $[\alpha]_D^{32} = +10.0$ ($c = 3.12$, $CHCl_3$) (available from Aldrich, $[\alpha]_D^{20} = +11.0$, ($c = 3.21$, $CHCl_3$)); **22**: $[\alpha]_D^{32} = +6.4$ ($c = 1.82$, $CHCl_3$) (*S* isomer: $[\alpha]_D^{20} = -7.6$, ($c = 2.0$, $CHCl_3$), F. A. Davis, M. S. Haque, T. G. Ulatowski, J. C. Towson, *J. Org. Chem.* **1986**, *51*, 2402); **25**: $[\alpha]_D^{32} = +12.8$ ($c = 1.66$, dioxane) (*R*-isomer: $[\alpha]_D^{20} = +13.2$ ($c =$ 1.51, dioxane), S.-S. Jew, H.-A. Kim, J.-H. Kim, H.-G. Park, *Heterocycles* **1997**, *46*, 65).
[22] J. A. Dale, H. S. Mosher, *J. Am. Chem. Soc.* **1973**, *95*, 512.

Directed Assembly of Periodic Materials from Protein and Oligonucleotide-Modified Nanoparticle Building Blocks**

So-Jung Park, Anne A. Lazarides, Chad A. Mirkin,* and Robert L. Letsinger*

In 1996 we reported a method for utilizing DNA and its synthetically programmable sequence recognition properties to assemble nanoparticles functionalized with oligonucleotides into preconceived architectures (Figure 1 B).[1] Since that initial report, our research group and many others have shown that this strategy[2–8] and off-shoots of it that rely on protein–receptor and antibody–antigen interactions[9–12] can be used to generate a wide range of architectures with many unusual and, in some cases, useful chemical and physical properties.

Since proteins and certain protein receptors can be functionalized with oligonucleotides, one, in principle, could immobilize such molecules onto oligonucleotide-modified nanoparticles and generate a new class of hybrid particles that exhibit the high stability of the oligonucleotide-modified particles but with molecular recognition properties that are dictated by the surface-immobilized protein or receptor rather than the DNA. Alternatively, one could functionalize a protein that has multiple receptor binding sites with receptor-modified oligonucleotides so that the protein receptor complex could be used as one of the building blocks, in place of one of the inorganic nanoparticles, in our original materials assembly scheme. Herein, we use 13-nm gold particles, streptavidin, and biotinylated DNA to explore these hypotheses (Figure 1 A) and some of the physical and chemical properties of the resulting new bioinorganic materials.

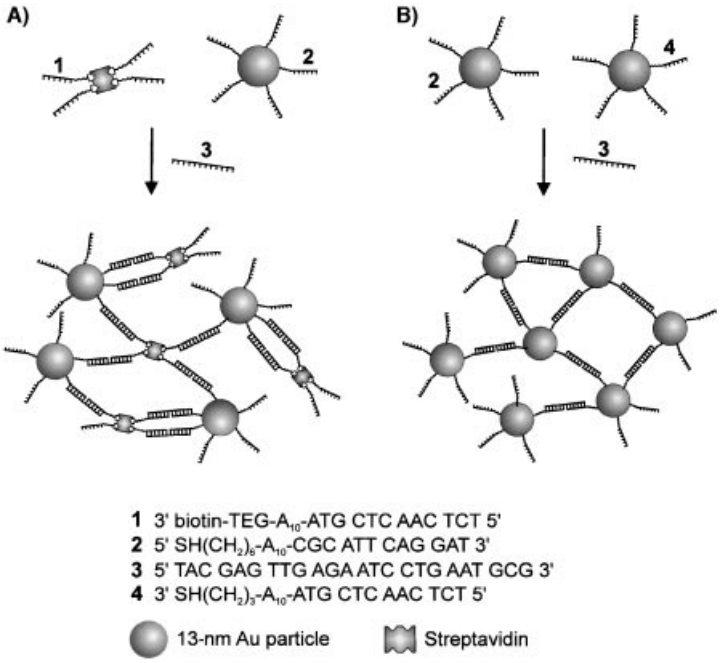

Figure 1. Schematic representation of DNA-directed assembly of Au nanoparticles and streptavidin. A) Assembly of oligonucleotide-functionalized streptavidin and Au nanoparticles (Au–STV assembly). B) Assembly of oligonucleotide-functionalized Au nanoparticles (Au–Au assembly). Note that **1** and **4** have the same DNA sequence.

The nanoparticle/protein assembly (Figure 1 A) reported herein relies on three building blocks: streptavidin complexed to four biotinylated oligonucleotides (**1**–STV), oligonucleotide-modified gold nanoparticles (**2**–Au), and a linker oligonucleotide (**3**) that has one half of its sequence complementary to **1** and the other half complementary to **2** (Figure 1). In a typical experiment, linker DNA (**3**; 10 μM, 21 μL) was introduced to a mixture of **2**–Au (9.7 nM, 260 μL) and **1**–STV (1.8 μM, 27 μL), or linker DNA **3** (10 μM, 21 μL) was premixed with **1**–STV (1.8 μM, 27 μL) and then the mixture was added to **2**–Au (9.7 nM, 260 μL) in 0.3 M phosphate-buffered saline (PBS) solution. Aggregates with similar properties could be formed by both methods, but premixing **3** and **1**–STV facilitates aggregate formation. Since a 13-nm gold particle is substantially larger than streptavidin ($4 \times 4 \times 5$ nm),[13, 14] a 1:20 molar ratio of Au nanoparticle to streptavidin was used to favor the formation of an extended polymeric structure rather than small aggregates comprised

[*] Prof. C. A. Mirkin, S.-J. Park, Prof. A. A. Lazarides
Department of Chemistry
and
Center for Nanofabrication and Molecular Self Assembly
Northwestern University
2145 Sheridan Road, Evanston, IL 60208-3113 (USA)
Fax: (+1) 847-467-5123
E-mail: camirkin@chem.nwu.edu
Prof. R. L. Letsinger
Department of Chemistry
Northwestern University
2145 Sheridan Road, Evanston, IL 60208-3113 (USA)
Fax: (+1) 847-491-2081
E-mail: rletsinger@chem.nwu.edu

[**] C.A.M. acknowledges DARPA, NSF, ARO, and NIH for support of this research. R.L.L. acknowledges the NIH. The DND-CAT Synchrotron Research Center is supported by E.I. Dupont de Nemours & Co., The Dow Chemical Company, the U.S. National Science Foundation through Grant DMR-9304725, and the State of Illinois through the Department of Commerce and the Board of Higher Education Grant IBHE HECA NWU 96. Use of the Advanced Photon Source was supported by the U.S. Department of Energy, Basic Energy Sciences, Office of Energy Research under Contract No. W-31-102-Eng-38.

Supporting information for this article is available on the WWW under http://www.angewandte.com or from the author.

of a few nanoparticles or a structure consisting of a single gold nanoparticle functionalized with a hybridized layer of streptavidin.

Interestingly, when **1**–STV, **2**–Au, and **3** were mixed at room temperature, no significant particle aggregation took place, even after three days, as evidenced by an unperturbed UV/Vis spectrum of the solution containing **1**–STV, **2**–Au, and **3**. However, raising the temperature of the solution (53 °C) to a few degrees below the melting temperature (T_m) of the DNA interconnects resulted in the growth of micrometer-sized aggregates (Figure 2A) and the characteristic red-shift and dampening of the Au plasmon resonance associated with particle assembly.[1] The transmission electron microscopy (TEM) image (Figure 2B) shows that the particles within the aggregates retain their physical shape prior to and after annealing, and shows that no particle fusion occurs. This result further demonstrates the stabilizing influence of the surface oligonucleotide layer. This requirement of thermal activation for initiating particle assembly is in contrast to the previously studied system involving two gold nanoparticle conjugates (Figure 1B) where, under very similar conditions, the oligonucleotide-modified gold particles assemble into aggregates within a few minutes upon adding linker DNA at room temperature.[1] This feature could be the result of: 1) the low collision probability in the Au–STV assembly system because of the lower DNA coverage on streptavidin (DNA:streptavidin = 4:1) relative to that on Au nanoparticles (DNA:particle ≈ 110:1),[15] or 2) initial formation of kinetic structures in which most or all of the DNA on a single streptavidin molecule binds to the DNA on a single particle. Aggregate formation could be facilitated by freezing the solution as well as heating it.[16] Finally, no aggregate formation was observed in a control experiment when a mixture of **1**–STV and **2**–Au (without **3**) was heated at 53 °C for 1 h. This observation demonstrates that aggregation in the three-component system (**1**–STV, **2**–Au, and **3**) is a DNA-driven process rather than one that results from nonspecific interactions.

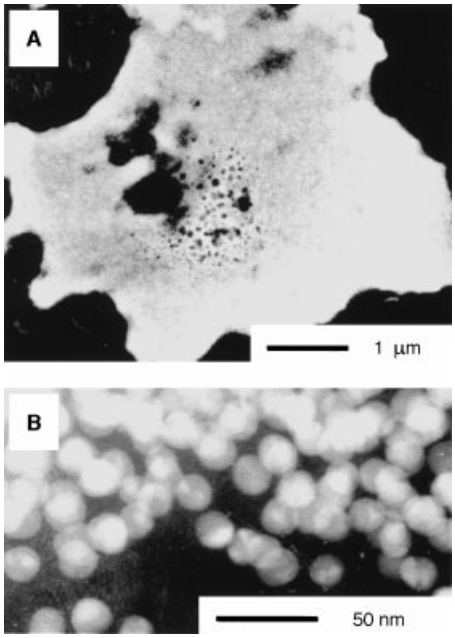

Figure 2. TEM images of 24-mer DNA linked aggregates of Au nanoparticles and streptavidin. A) Low magnification image showing an entire aggregate. B) High magnification image of a portion of the aggregate.

Melting experiments, based on UV/Vis spectroscopy, were performed on the streptavidin/nanoparticle aggregates (Figure 3A). Upon heating the aggregates, the extinction coefficient at 520 nm initially decreases, which results in a dip in the melting curve, and then abruptly increases when DNA melting takes place and the particles are dispersed. This dipping behavior has been observed in the pure gold nanoparticle system and has been attributed to aggregate growth prior to melting, that is, a type of aggregate "ripening".[5] After DNA melting has occurred, the Au plasmon resonance is centered at 520 nm, which is characteristic of dispersed 13-nm particles. These experiments further demonstrate that sequence-specific hybridization events, rather than nonspecific interactions, are effecting the particle/protein assembly and that the aggregation process is completely reversible.

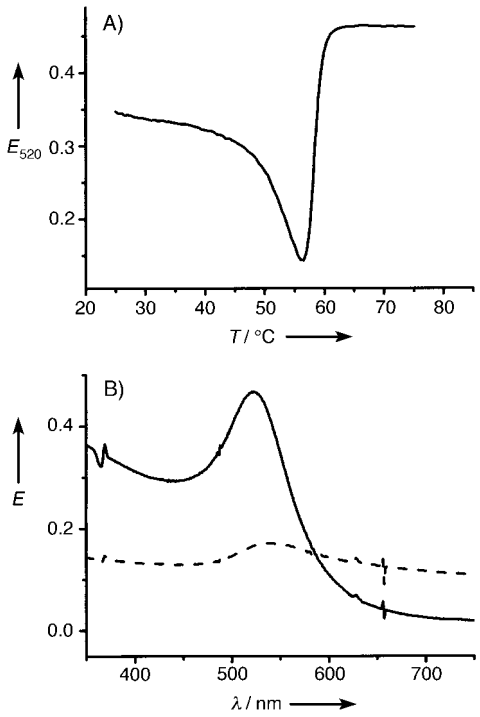

Figure 3. A) Thermal dissociation curve of the 24-mer DNA linked aggregates consisting of Au nanoparticles and streptavidin. The extinction coefficient at 520 nm was monitored as a function of temperature while stirring the solution. B) UV/Vis spectra of the solution measured before (– – – 56 °C) and after melting of the DNA (—— 65 °C).

An Au nanoparticle/protein assembly could also be formed through streptavidin/biotin interactions instead of hybridization-induced assembly. For example, in a typical experiment **1** (0.24 mM, 1.3 μL), **3** (10 μM, 32 μL), and **2**-modified nanoparticles (Au nanoparticle concentration: 9.7 nM, 260 μL) were mixed in 0.3 M PBS solution to generate biotin-modified Au particles. The mixture was heated at 60 °C for 10 min and then cooled to room temperature to facilitate hybridization. The solution containing **1**, **3**, and **2**-modified Au nanoparticles

  1433-7851/01/4015-2910 $ 17.50+.50/0

was added after 24 h to streptavidin (10 μM, 4.2 μL) in 0.3 M PBS, and heated to 50 °C to form the nanoparticle aggregates. The color of the solution turned purple indicating aggregate formation had occurred, and the aggregates could be disassembled to **2**-modified Au particles, **1**-modified streptavidin, and **3** by raising the temperature of the solution above the melting temperature (65 °C).

Small-angle X-ray scattering (SAXS)[7, 17, 18] data were collected for aggregates formed from the Au nanoparticle and streptavidin building blocks (**1** – STV, **2** – Au) and two different lengths of DNA linker (24-mer (**3**) and 48-mer), and they were compared to those for aggregates based on an Au – Au assembly with the same linking oligonucleotides (**2** – Au, **4** – Au, 24-mer linker (**3**), 48-mer linker; Figure 4). The 48-mer

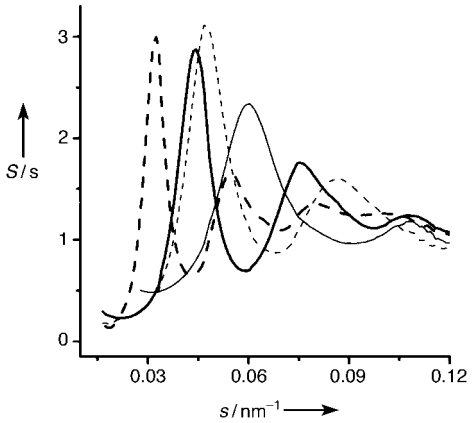

Figure 4. Structure factors of the DNA linked Au – STV (—— 24-mer-linked, – – – 48-mer-linked) and Au – Au assemblies (—— 24-mer-linked, – – – 48-mer-linked) from SAXS patterns. The aggregate solutions were heated at 47 °C for 30 min to obtain thermodynamic structures. The SAXS experiments were performed at the Dupont – Northwestern – Dow Collaborative Access Team (DND-CAT) Sector 5 of the Advanced Photon Source, Argonne National Laboratory with X-rays of wavelength 1.24 Å. Samples were placed in 1.2-mm flat cells between Kapton windows. The magnitude, $s(=q/2\pi)$, of the scattering vector is $2\sin(\theta)/\lambda$, where 2θ is the scattering angle and λ is the wavelength of the incident radiation. The scattered intensity $I(s)$ is approximately proportional to the structure factor $S(s)$ as follows: $I(s) \approx F^2(s)S(s)$, where $F^2(s)$ is the scattered intensity associated with the dispersed DNA-modified Au nanoparticles without linker. The scattering from streptavidin and DNA is negligible relative to the scattering from the Au nanoparticles.

linker was a duplex consisting of 5′TACGAGTTGAGACCGTTAAGACGAGGCAATCATGCAATCCTGAATGCG and 3′GGCAATTCTGCTCCGTTAGTACGT (the duplex region is underlined) with 12-mer sticky ends that are complementary to **1** and **2**. For design of the SAXS experiments, A_{10} spacers in **1**, **2**, and **4**, which were used in the above experiments to enhance the possibility of DNA hybridization,[15] were removed to create a more rigid system for use in the SAXS experiments. The aggregates linked by DNA showed relatively well-defined diffraction peaks, and the Au – STV aggregates exhibited diffraction peaks at smaller s values than the Au – Au aggregates formed from the same linker. This observation suggests a larger interparticle distance between the Au centers in the Au – STV system. Furthermore, the diffraction peaks shifted to smaller angles when 48-mer DNA was used as a linker instead of the 24-mer for both the Au – Au and Au – STV assemblies (Figure 4).

The pair distance distribution function (PDDF) $g(r)$ has been calculated from the SAXS patterns using Equation (1), where $q = (4\pi/\lambda)\sin(\theta)$ and ρ is the particle number density.[17, 18]

$$g(r) = 1 + (1/2\pi^2\rho r)\int q(S(q) - 1)\sin(qr)\mathrm{d}q \quad (1)$$

$g(r)$ gives the probability of finding a second particle as a function of distance r from a chosen particle. The nearest neighbor interparticle Au – Au distances (center to center distance) obtained from the PDDFs are 19.3, 25.4, 28.7, and 40.0 nm for the 24-mer-linked Au – Au, 48-mer-linked Au – Au, 24-mer-linked Au – STV, and 48-mer-linked Au – STV assemblies, respectively. A comparison of the interparticle distances for the Au – STV system and the Au – Au system clearly shows that the Au – STV assembly has the anticipated Au nanoparticle/streptavidin periodicity and that the two components (Au nanoparticle and streptavidin) are well separated by rigid DNA duplex linkers.

This study is important for the following reasons. 1) It demonstrates that the DNA-directed nanoparticle assembly method is extendable to protein-based structures, in addition to the inorganic nanoparticles studied thus far. Indeed, this is the first report demonstrating the reversible DNA-directed assembly of Au nanoparticles and a protein-based structure functionalized with DNA into macroscopic, periodic architectures. Other research groups have used a different strategy for preparing linear structures from 1.4-nm particles, DNA, and streptavidin.[9, 19, 20] 2) It is well known that many proteins, including streptavidin, will adsorb onto the surface of colloidal gold to form strongly bound complexes. Our experiments demonstrate the stabilizing influence of the high-density DNA layers on the nanoparticle surfaces and their resistance to streptavidin adsorption in the absence of hybridization. Therefore, they point towards a method for specifically immobilizing protein structures on nanoparticle surfaces through very specific interactions in a way that will not substantially perturb the activity of the protein. Particles with surface-adsorbed proteins have played an important role in immunochemistry,[21] and the development of stable protein/particle conjugates where the protein does not directly interact with the nanoparticle surface could lead to improved nanoparticle probes for histochemical studies and immunoassays.

Experimental Section

The methods for preparing oligonucleotide-modified 13-nm Au particles (**2** – Au) and linker DNA (**3**) are reported elsewhere.[2] **2** – Au and **3** were stored in a mixture of 0.3 M NaCl and 10 mM phosphate (pH 7) buffer (0.3 M PBS) prior to use. Biotin-modified DNA (**2**) was synthesized from Biotin TEG CPG support (Glen Research) and purified by literature methods.[2, 22] Streptavidin was purchased from Sigma and dissolved in 20 mM tris(hydroxymethyl)aminomethane (Tris) buffer (30 μM, pH 7.2). To make the streptavidin/DNA conjugate (**1** – STV), streptavidin was treated with **1** (8 equiv) in a mixture of 20 mM Tris (pH 7.2) and 0.2 mM ethylenediaminetetraacetate (EDTA) buffer solution at room temperature for 2 h on a shaker. Mixtures with different ratios of streptavidin to DNA (1:0.4, 1:1, 1:4) were also prepared for HPLC analysis. The streptavidin/DNA

  1433-7851/01/4015-2911 $ 17.50+.50/0

conjugates were separated from excess DNA by ion-exchange HPLC starting with 20 mM Tris (pH 7.2) and then using a 0.5 % min^{-1} gradient of a solution of 20 mM Tris and 1M NaCl at a flow rate of 1 mL min^{-1}, while monitoring the UV signal at 260 and 280 nm. The 1:0.4 streptavidin:DNA mixture showed two peaks at 45 and 56 min, while the 1:1 mixture showed four peaks at 45, 56, 67, and 71 min, which correspond to the 1:1, 2:1, 3:1, and 4:1 oligonucleotide:streptavidin complexes, respectively. The 1:4 mixture showed four peaks at the same positions but with increased intensity of the third (67 min) and fourth (71 min) peaks. The HPLC chromatogram of the 1:8 streptavidin:DNA mixture showed two main peaks, one at 59 min for recovered DNA and the other at 71 min for the 4:1 oligonucleotide:streptavidin complex. In addition, a shoulder at 67 min, assigned to the 3:1 complex, was also present. Purified streptavidin–biotinylated-DNA conjugates were concentrated and dispersed in 0.3 M PBS by ultrafiltration (centricon 30). Aggregates for TEM, thermal denaturation experiments, and SAXS measurements were prepared by freezing the solution containing **1**–STV, **2**–Au, and **3** in dry ice for 10 min, and thawing to facilitate hybridization prior to the measurement.

Received: February 26, 2001
Revised: May 22, 2001 [Z16692]

[1] C. A. Mirkin, R. L. Letsinger, R. C. Mucic, J. J. Storhoff, *Nature* **1996**, *382*, 607.
[2] J. J. Storhoff, R. Elghanian, R. C. Mucic, C. A. Mirkin, R. L. Letsinger, *J. Am. Chem. Soc.* **1998**, *120*, 1959.
[3] R. C. Mucic, J. J. Storhoff, C. A. Mirkin, R. L. Letsinger, *J. Am. Chem. Soc.* **1998**, *120*, 12674.
[4] G. P. Mitchell, C. A. Mirkin, R. L. Letsinger, *J. Am. Chem. Soc.* **1999**, *121*, 8122.
[5] J. J. Storhoff, A. A. Lazarides, C. A. Mirkin, R. L. Letsinger, R. C. Mucic, G. C. Schatz, *J. Am. Chem. Soc.* **2000**, *122*, 4640.
[6] T. A. Taton, R. C. Mucic, C. A. Mirkin, R. L. Letsinger, *J. Am. Chem. Soc.* **2000**, *122*, 6305.
[7] S.-J. Park, A. A. Lazarides, C. A. Mirkin, P. W. Brazis, C. R. Kannewurf, R. L. Letsinger, *Angew. Chem.* **2000**, *112*, 4003; *Angew. Chem. Int. Ed.* **2000**, *39*, 3845.
[8] T. A. Taton, C. A. Mirkin, R. L. Letsinger, *Science* **2000**, *289*, 1757.
[9] C. M. Niemeyer, W. Burger, J. Peplies, *Angew. Chem.* **1998**, *110*, 2391; *Angew. Chem. Int. Ed.* **1998**, *37*, 2265.
[10] W. Shenton, S. A. Davis, S. Mann, *Adv. Mater.* **1999**, *11*, 449.
[11] S. Connolly, D. Fitzmaurice, *Adv. Mater.* **1999**, *11*, 1202.
[12] M. Li, K. W. Wong, S. Mann, *Chem. Mater.* **1999**, *11*, 23.
[13] P. C. Weber, D. H. Ohlendorf, J. J. Wendoloski, F. R. Salemme, *Science* **1989**, *243*, 85.
[14] N. M. Green, *Methods Enzymol.* **1990**, *184*, 51.
[15] L. M. Demers, C. A. Mirkin, R. C. Mucic, R. A. Reynolds, R. L. Letsinger, R. Elghanian, G. Viswanadham, *Anal. Chem.* **2000**, *72*, 5535.
[16] R. Elghanian, J. J. Storhoff, R. C. Mucic, R. L. Letsinger, C. A. Mirkin, *Science* **1997**, *277*, 1078.
[17] A. Guinier, A. Fournet, *Small Angle Scattering of X-rays*, Wiley, New York, **1955**.
[18] B. A. Korgel, D. Fitzmaurice, *Phys. Rev. B* **1999**, *59*, 14191.
[19] C. M. Niemeyer, T. Sano, C. L. Smith, C. R. Cantor, *Nucleic Acids Res.* **1994**, *22*, 5530.
[20] C. M. Niemeyer, L. Boldt, B. Ceyhan, D. Blohm, *Anal. Biochem.* **1999**, *268*, 54.
[21] M. A. Hayat, *Colloidal Gold: Principles, Methods, and Applications*, Academic Press, San Diego, **1991**.
[22] T. Brown, D. J. S. Brown in *Oligonuclieotides and Analogues* (Ed.: F. Eckstein), Oxford University Press, New York, **1991**.

Ruthenium-Catalyzed One-Step Transformation of Propargylic Alcohols into Alkylidene Cyclobutenes: X-ray Characterization of an Ru(η^3-cyclobutenyl) Intermediate**

Jacques Le Paih, Sylvie Dérien, Christian Bruneau, Bernard Demerseman, Loïc Toupet, and Pierre H. Dixneuf*

Among unsaturated small cycles, cyclobutenes are especially useful as building-block precursors. They allow the general in situ generation of reactive functional 1,3-diene skeletons,[1] a key process for the synthesis of phytotoxic natural products[2] or polycyclic derivatives.[3] Cyclobutenes were also shown to be precursors of 1,5-dienes for access to pheromones by ring-opening catalysis.[4] The most general methods to produce simple cyclobutenes are based on the [2+2] cycloaddition of C≡C and C=C bonds, either photochemically[5] or with Lewis acids[6] and metal-based[7] catalysts, and on the zirconocene-catalyzed reaction of alkynyl halides with Grignard reagents.[8] In contrast, the access to alkylidenecyclobutenes is not straightforward and occurs by intramolecular thermal coupling of 1,5-diynes[9] or copper-mediated cyclization from 1,4-enynes.[10]

We have recently shown that the catalyst precursor [Cp*RuCl(cod)] (Cp* = C_5Me_5, cod = 1,5-cyclooctadiene) promotes the head-to-head coupling of two terminal alkynes, via a chelating biscarbene–ruthenium intermediate, which, upon addition of a carboxylic acid produces 1-acyloxybuta-1,3-dienes [Eq. (1)].[11] We now report that the same electron-rich precatalyst [Cp*RuCl(cod)] activates propargylic alcohols in a novel manner in the presence of a carboxylic acid. It leads to the one-step catalytic head-to-head cyclodimerization

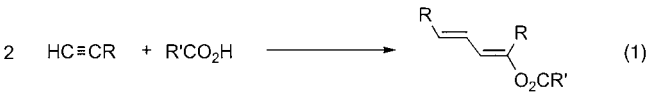

(1)

[*] Prof. P. H. Dixneuf, Dr. J. Le Paih, Dr. S. Dérien, Dr. C. Bruneau, Dr. B. Demerseman
Institut de Chimie de Rennes
UMR 6509 CNRS-Université de Rennes
Organométalliques et Catalyse
Campus de Beaulieu, 35042 Rennes (France)
Fax: (+33) 2-99286939
E-mail: pierre.dixneuf@univ-rennes1.fr
Dr. L. Toupet
Groupe Matière Condensée et Matériaux
UMR 6626 CNRS-Université de Rennes
Campus de Beaulieu, 35042 Rennes (France)

[**] This work was supported by the CNRS and the Ministère de la Recherche. The authors are grateful to the latter for a PhD grant to J. LP. The authors wish to thank the European Cost Program D17/003/00 and the Région Bretagne for financial support. They are also grateful to A. Bondon for helpful assistance in NMR analysis.

Supporting information for this article is available on the WWW under http://www.angewandte.com or from the author.

  1433-7851/01/4015-2912 $ 17.50+.50/0